JOURNAL OF MATERIALS SCIENCE 37 (2002) 389–395

Crystalline structure of a liquid crystal forming ligated twin

A. J. WADDON, T. P. RUSSELL
Department of Polymer Science and Engineering, University of Massachusetts, Amherst, MA 01003, USA
E-mail: waddon@polysci.umass.edu

The solid state crystalline structure of a low molecular weight ligated dimer twin has been examined by TEM and x-ray diffraction methods. In this material each twin consists of a short, central rigid three phenylene ring segment, with short alkane tails attached at both ends; this is joined to its twin by a connecting methyl group. This was found to form a layered structure of period ~35 Å in which the molecule adopts an extended conformation wherein both the alkane tails and the rigid units form their own sub-layers, imparting a mosaic morphology to the system. © *2002 Kluwer Academic Publishers*

1. Introduction

Low molecular weight liquid crystals comprised of sequences of flexible, aliphatic segments connected to a stiff, rigid moeity are interesting materials from both fundamental and practical viewpoints. Such materials can display ferroelectric and antiferroelectric properties leading to their use in electro-optical devices. These particular compounds are typically formed by attaching pendant alkyl chains to a stiff, mesogenic, rod-like unit to form essentially short chain triblock materials. It is also possible to covalently join two such units by covalent bridging linkages to form so-called ligated twin liquid crystals [1–3]. This article is concerned with the crystal structure and conformation of such a material.

The material of interest is shown in Fig. 1a in one of the two possible extended chain configurations. Each half of the ligated twin consists of a central stiff unit, comprised of a diphenyl group separated from a third phenyl ring by an ester group, and two short chain alkyl units attached on either side of the mesogen. The twins are linked at equivalent positions on the central mesogen by a bridging $-CH_2-$ unit. Accordingly, the molecule is symmetric around this pivotal methyl group.

The conformation of the molecule is of course dependent upon the configuration of the bonds around the bridge. In the crystalline state it is reasonable to assume that the molecule will adopt a symmetric conformation. On one extreme is the conformation shown in Fig. 1a (termed the U conformation) where the two halves of the molecule lie exactly parallel. Of course, since the methyl bond angle is 109°, the two halves of the molecule cannot lie parallel if the bridging phenylene rings are co-planar. However, consideration of this also shows that slight rotation of these phenylenes about the CH_2 group allows the two rigid halves of the molecule to then achieve parallelity.

The other extreme is formed by a rotation around the bridging methyl to form the conformation shown schematically in Fig. 1b (the S conformation). With the planes of the bridging phenylenes inclined at approximately 110° (calculated using accepted values of bond angles and bond lengths) the attached ester groups point in exactly opposite directions (anti-parallel). In either case it is simple to calculate the approximate extended length of the chain. It is most convenient to consider each half of the molecule as being comprised of two flexible blocks attached on either side of a rigid block. Using accepted bond lengths and angles the end to end distance for the U and S conformers are approximately 33 and 47 Å respectively.

In this work the principal structural features of this molecule in the solid phase were investigated, in particular whether the S or U conformation is preferred. By combined x-ray and electron diffraction studies it is shown that the alkyl and aromatic segments separate into sub-layers.

2. Experimental

The material was provided in the form of solid aggregates rather than as a powder. These aggregates were sheet-like in appearance suggesting some inherent anisotropy. The aggregates were investigated by small angle x-ray scattering (SAXS) with the x-ray beam parallel to the plane of the sheets using an evacuated pinhole collimated Statton camera at appropriate camera lengths with Ni filtered Cu K_α radiation. Wide angle x-ray diffraction (WAXD) characteristics of a ground powder were obtained using a Siemens D500 diffractometer in normal/transmission mode with 0.3° slits with the sample mounted in a glass x-ray capillary.

A small quantity of the material was dissolved by gentle heating in hexane. On cooling to room temperature crystallization occurred, leaving a suspension of crystals dispersed in solvent. Some of this was deposited on a microscope slide, allowed to dry and examined in a polarizing light microscope.

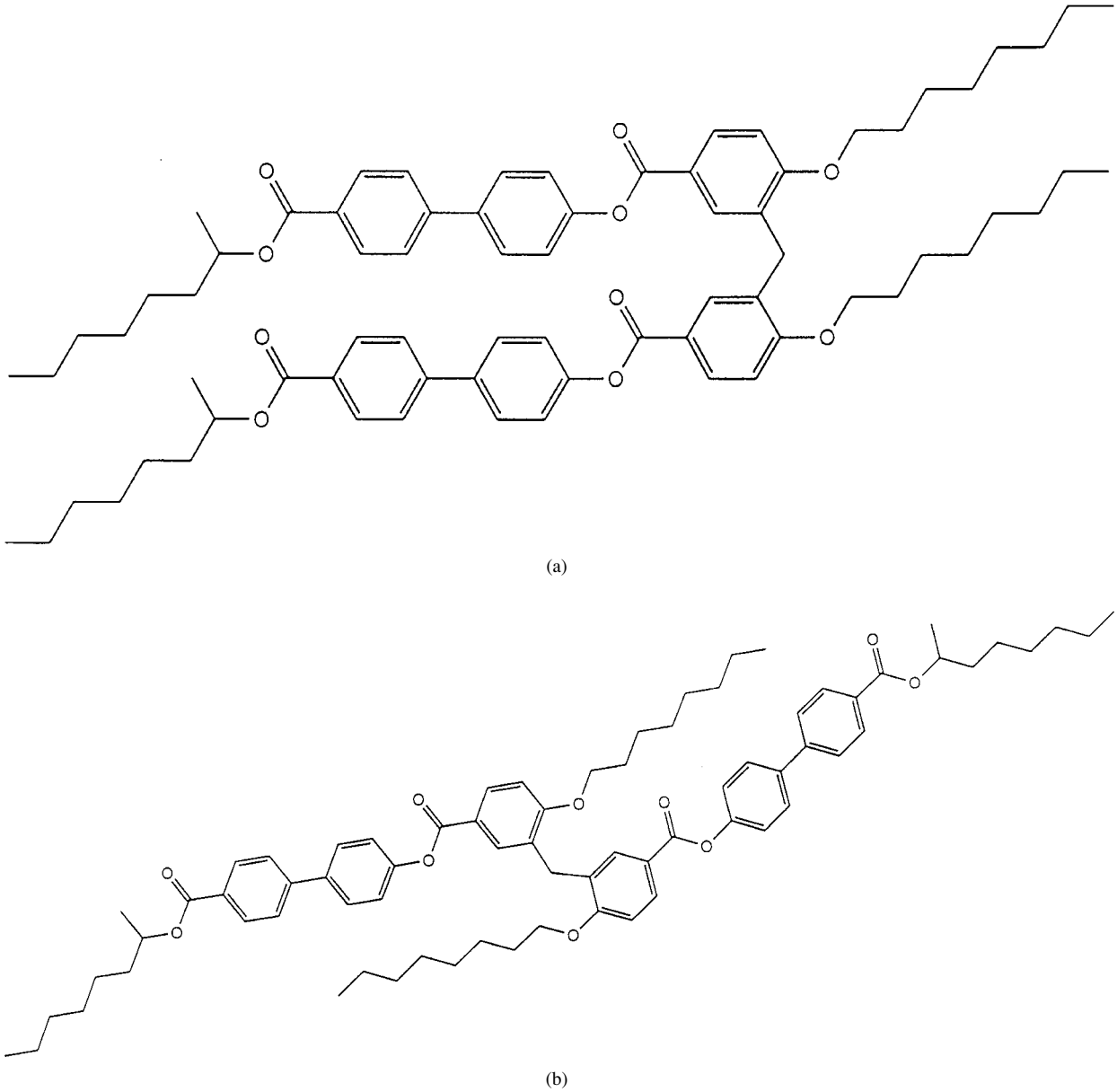

Figure 1 Schematics of ligated twin in chain extended conformations. (a) U conformer; rotation about the bridging CH_2 tilts planes of bridging phenylene rings and brings arms of the molecule parallel; (b) S conformer, rigid units lie anti-parallel when planes of phenylene rings are inclined at $\sim 110^\circ$.

For examination in the transmission electron microscope (TEM) the suspension was allowed to dry on carbon coated copper TEM grids. Subsequently the samples were examined in a Jeol 100CX operating at an accelerating voltage of 100 kV.

3. Results

The SAXS pattern (Fig. 2) of the as-received crystalline aggregate showed at least five sharp, well defined orders of reflections with the maximum intensity at right angles to the plane of the crystal mat, (although higher orders are not expected to reproduce well). The *d* spacings for these reflections are listed in Table I. The fundamental repeat period corresponding to these reflections is 36.5 Å. This is identified with the long period of the crystals in the mat. The large number and sharpness of the reflections indicates that the spacing is very well defined and the packing of the layers highly regular.

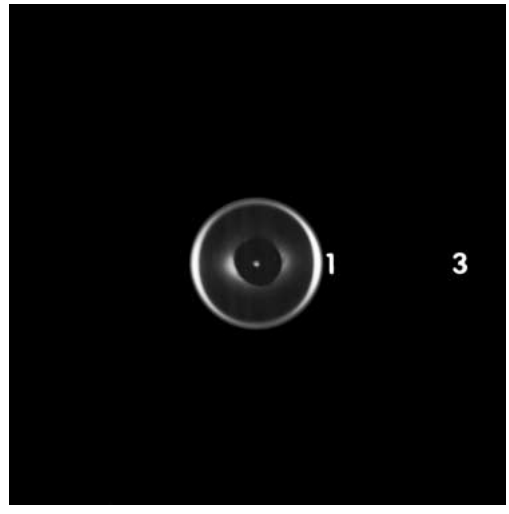

Figure 2 SAXS pattern of as received aggregate. Plane of mat vertical. Orders 1 and 3 are marked on the figure. Even orders appear unusually weak.

It is also striking that the intensities of the 2nd and 4th orders in the SAXS pattern are unusually weak. This is a result of a discontinuity in the electron density profile at some fraction of the lamellar thickness. Details of this need to be considered more closely, (e.g. by taking the Fourier transform of the scattering profile) and may be expected to yield details of the electron density profile as a function of depth through the layer.

The diffractogram, Fig. 3, also shows the 3rd order of the layer spacing (at 2θ of 7.2°). Prominent in this trace are higher angle (and rather broad) peaks at 2θ of 17.3° (5.13 Å) and 22.6° (3.93 Å). In addition, there are a family of at least three peaks between 10° and 14° (corresponding to spacings of 7.97, 7.20 and 6.56 Å) and a sharp peak at 24.6° (3.61 Å). Most significantly, there are no signs of signals from an alkane lattice (in any of the known crystal modifications), suggesting that there has been no large scale crystallization of the alkane tails into a separate lattice. There is, however, evidence of a substantial amorphous halo.

Fig. 4, shows two possible packing schemes for the two conformations. As can be seen either conformation yields a layer spacing close to the observed spacing. Both arrangements provide for the formation of layers of alkane material within the structure. The close correspondence of the SAXS periodicity with the extended chain lengths also means that there cannot be substantial tilting of the molecules with respect to the layer normal, whichever scheme is correct. Nevertheless, there are important differences between these schemes. Scheme I (U conformation) requires the rigid ligands on the same molecule to be adjacent and, accordingly, their maximum separation cannot exceed the length determined by the covalent bonds. This conformation also permits the maximum aggregation of the alkanes into separate layers with alkane layers formed by both types of alkane tails. In Scheme I each alkane tail in an alkane layer is linearly connected to an aryl group in an adjoining aryl layer. Therefore, the lateral cross-sectional area occupied per alkane group will be approximately equal to that occupied by an aryl group.

In contrast, Scheme II (S conformation) provides only for alkane layers formed by inter-digitation of the tails attached via the ester links. The other alkane tails are located between aryl segments in the neighboring aryl layer. Particularly noteworthy in this scheme, in any alkane layer only half the alkane segments are connected to aryl segments in a given neighboring (say the lower) aryl layer. Therefore, the lateral area occupied by each aryl segment must be twice that occupied per akyl segment.

Examination between crossed polars showed the crystals to be highly birefringent and needle-like, extinction occurring when the vibration direction of the incident light was either parallel or perpendicular to the needle axis. The shift in polarization colors when a wavelength plate was inserted between polars at 45° to the vibration directions indicated that the direction of highest refractive index was perpendicular to the long direction of the crystals. Following usual conventions the crystals would therefore be termed as negatively birefringence. This is consistent with the molecular axis also lying essentially perpendicular to the long axis of the crystals.

Bright-field electron micrographs of the crystals are shown in Fig. 5. These show microscopic lath-like features of length ranging from ~6–30 μm and width 0.12–0.25 μm. In places there is clear evidence of aggregation of the laths into larger, acicular entities, and it is reasonable to conclude that the features seen in optical microscopy are a result of similar aggregation but on a slightly larger scale.

The electron diffraction patterns from these crystals are enormously rich and informative and, therefore, we will describe them with some care. An example of one such pattern is shown in Fig. 6. There were two features immediately obvious from this pattern. First, a single crystal spot pattern was evident. This is a zone axis

TABLE I "*d*-spacings" from SAXS

n	*d* (Å)
1	36.5
2	18.25
3	12.12
4	9.13
5	7.3

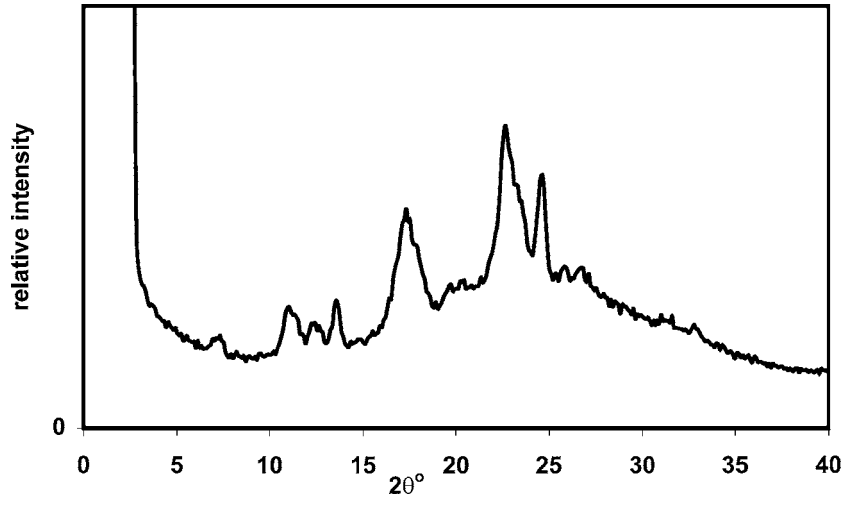

Figure 3 Diffractometer trace from ground powder of as-received material.

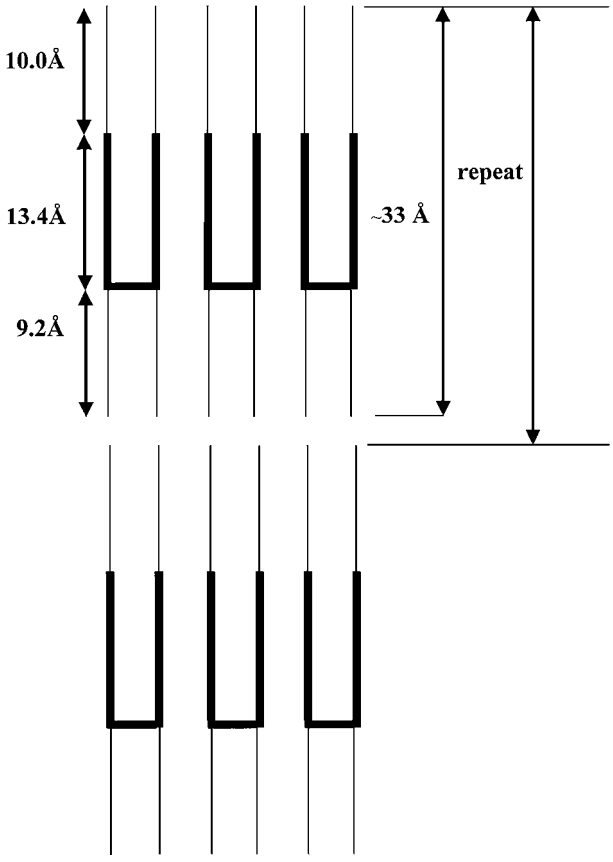

(a)

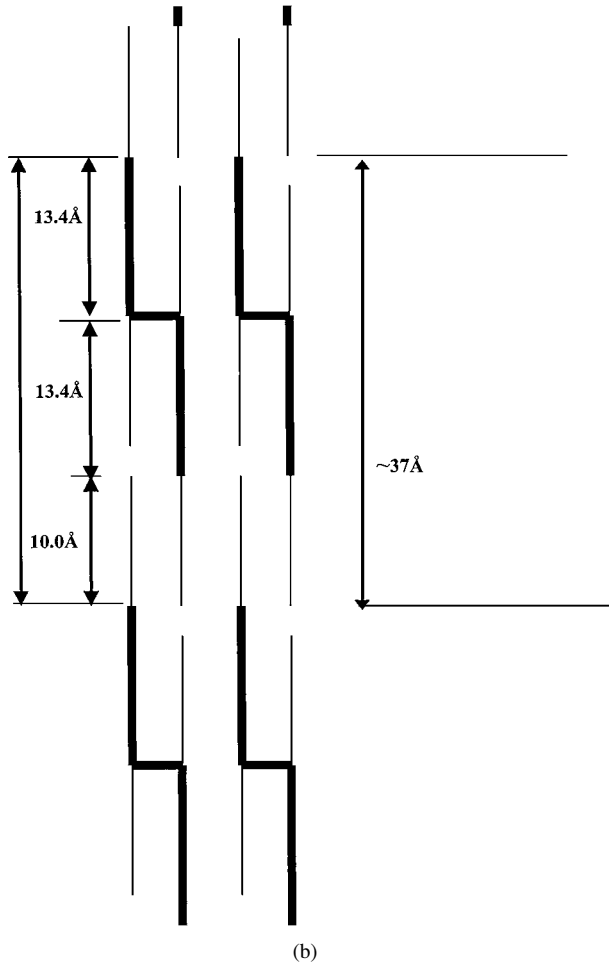

(b)

Figure 4 Possible schemes of packing which would give a layer repeat approximately equivalent to the experimentally determined value: (a) U conformer; (b) S conformer.

TABLE II Alkane spacing from electron diffraction, Å

*hk*0	Dimer	Polyethylene [4]	% Expansion
110	4.21	4.10	2.7
200	3.77	3.70	1.9
020	2.54	2.47	2.8
Area per chain, Å^2	19.15	18.28	4.8

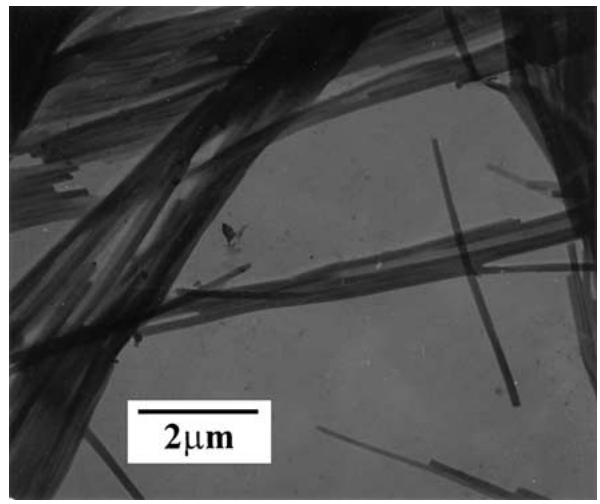

Figure 5 Transmission electron micrograph of crystals. Solution grown from hexane.

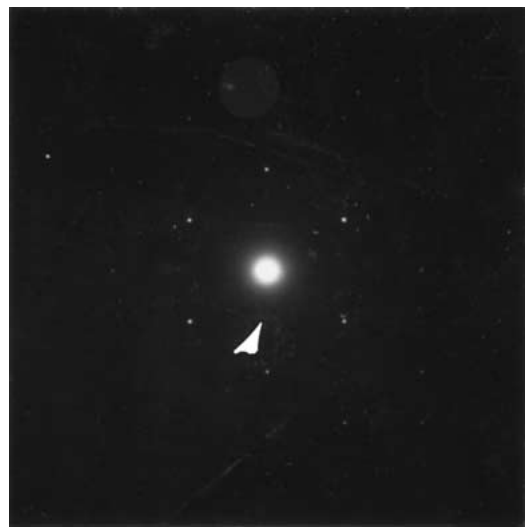

Figure 6 Electron diffraction pattern. The spots are the *hk*0 reflections of an orthorhombic alkane lattice. The weaker, arced reflections (arrowed) arise from the packing of the aryl sequences. The small angle reflection at ~35 Å (not visible on print) is horizontal.

pattern from a two dimensional orthorhombic crystal. These are, therefore, indexed as *hk*0s (see Table II). Second, a very low angle, single crystal reflection (not visible on the print) was observed. Defocussing of the central spot showed that this low angle reflection was located perpendicular to the lath direction. Measurement of this reflection on other similar patterns gave a spacing of ~35 Å.

The spacings for the orthorhombic reflections are listed in Table II where they are compared with the literature values for polyethylene (PE) [4]. The close correspondence between the dimer reflections listed in

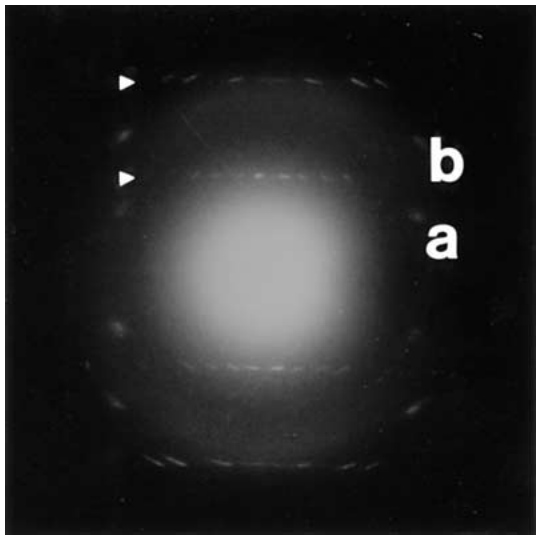

(a)

(b)

Figure 7 Non-alkane electron diffraction patterns (a) shows (i) signals on layer lines with an 8.3 Å periodicity (ii) non-layer reflections **a** and **b**; (b) shows equatorial reflection at ∼35 Å. Needle axis vertical. Patterns (a) and (b) from different regions but shown in correct orientational correlation.

Table II and PE allows us to reasonably attribute these to some limited crystallization of the alkane tails in the dimer, despite the absence of alkane signals in WAXD. The slight expansion of the spacings compared with the usual alkane lattice can be reasonably accounted for by the physical constraints of attachment to the aromatic central core. The crystallization of the alkane units in the olefinic lattice is therefore affected by the presence of the rigid units. Note that the distortion is asymmetric, being less along $\mathbf{a}_{\text{alkane}}$ than along $\mathbf{b}_{\text{alkane}}$.

Other crucial, albeit weaker, reflections are also evident. Some of these weaker reflections, arrowed in Fig. 6, are enhanced in Fig. 7a in which the alkane reflections are absent. The small angle reflection at 35 Å was located equatorially (horizontally) just outside of the main beam and exhibited an orientational correlation with the other reflections in Fig. 7a, indicating they did indeed originate from the same morphological features. A similar reflection from a different area is printed more clearly in Fig. 7b. However, while the low angle reflection is the spot of a single diffracting entity, the other reflections are noticeably arced, a result of diffraction from a population of crystallites with a distribution of orientations, i.e. the "single diffracting entity" producing the low angle signal is a polycrystalline

TABLE III Electron diffraction reflections showing fiber symmetry with 8.3 Å periodicity

Reflection	Spacing, Å
A1 (1st layer)	8.27
A2	7.91
A3	7.21
A4	6.56
A5	3.37
B1 (2nd layer)	4.14
B2	4.02
B3	3.77
B4	3.60
C1 (4th layer)	2.07

aggregate. These patterns have the characteristics of conventional fiber patterns with the needle axis lying parallel to that of the fiber. Consequently the morphology can be described as an ensemble of diffractors (of thicknesses ∼35 Å) with one common axis (the needle axis) but which are randomized (i.e. rotated) around this axis.

The fiber pattern in Fig. 7a exhibits a layer periodicity of ∼8.3 Å parallel to the lath axis with numerous sharp reflections visible on the 1st, 2nd and 4th layer lines. The 1st and 2nd layer lines are arrowed on the print (Fig. 7a) and the spacings of the individual reflections are listed in Table III. From consideration of the spacings, the 1st layer reflections A2, A3 and A4 can be identified as the signals seen in WAXD between 2θ of 10 and 14° (Fig. 3). The 1st layer line reflections are also those arrowed on Fig. 6. (This would suggest that the 200_{alkane} is parallel to the fiber axis. This, however, is coincidental; other examples were found not showing this correlation.)

The above pattern (Fig. 7a) which corresponds to a layer periodicity of ∼8.3 Å will be referred to as Pattern I. However, the following additional features can also be identified. Comparatively diffuse reflections at 5.13 and 4.00 Å at angles of 67.5° and 48.5° respectively to the lath axis were observed. These are marked as reflections **a** and **b,** respectively on Fig. 7a and can be identified as the same reflections as the two prominent WAXD signals at 17.3° (5.13 Å) and 22.6° (3.93 Å), (see Fig. 3). These signals share the same fiber axis as the reflections of Pattern I but do not lie on the same layer lines. Moreover, these reflections are very diffuse in nature. This will be referred to as Pattern II.

4. Discussion

The 35 Å reflection in electron diffraction is very close to the SAXS layer spacing and is clearly the same reflection. It is also clear from WAXD that there is no significant crystallization of the alkane tails into a separate lattice, although from electron diffraction it is apparent that there is some, very limited, crystallization of an expanded alkane structure. Therefore, the essential features of the electron diffraction Patterns I and II must have their origins in the crystal structure of the rigid component. It is also clear that Patterns I and II reflect different aspects of the rigid component's structure and that the 5.13 and 4.00 Å reflections of Pattern II

TABLE IV Area per chain of rigid component of dimer in crystal compared to other structurally similar materials

	Rigid repeating unit	Area per chain, Å^2
Dimer	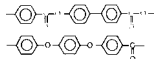	22.7
PEEK [5]	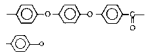	22.7
Poly(phenylene oxide) [6]		22.4

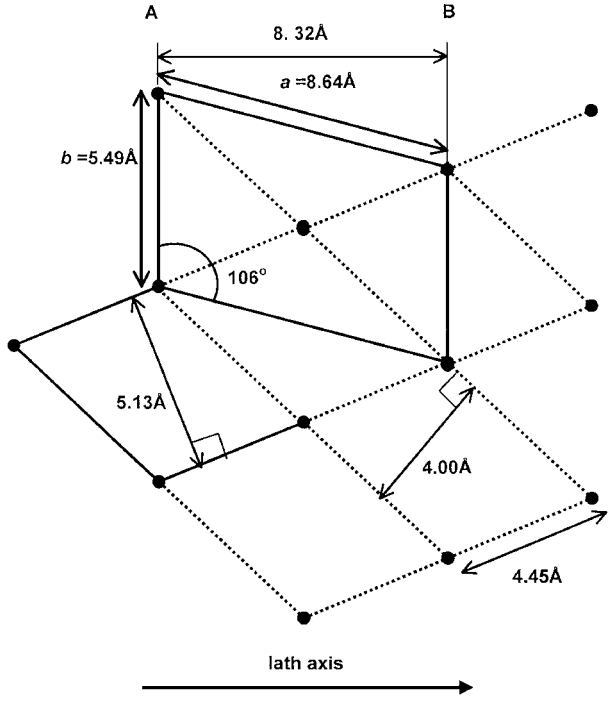

Figure 8 Proposed monoclinic cell of aryl sequences in chain axis projection.

are obviously the same prominent reflections identified by x-ray diffraction of the bulk, Fig. 3. Careful consideration of Pattern II shows that it may be derived reasonably well from a 2 dimensional monoclinic cell. While the fit between cell dimensions and diffraction data may need refinement, the cell of Fig. 8 is correct in its essential dimensions. This corresponds to a projection along the molecular or ***c*** axis of a two chain monoclinic cell with $\boldsymbol{a} = 8.64$, $\boldsymbol{b} = 5.49$ Å and $\gamma = 106^\circ$ (our assignments). In Fig. 8 the needle axis is horizontal and perpendicular to ***b***. The reflections of Patterns II at 5.13 and 4.00 Å can be indexed as $\bar{1}10$ and 110, respectively. It is also noteworthy that four spots are found for each of the $hk0$ reflections rather than the two expected for a single lattice. Thus, the actual pattern obtained is consistent with diffraction from an ensemble of crystals, related by a common b axis direction which lies perpendicular to the lath axis and also in the plane of the lath. Since $\gamma \neq 90^\circ$, there will be two sets of crystals having a oriented at $\pm 16^\circ$ to the lath axis (in a "twinned relationship"), leading to the four reflections for both $\bar{1}10$ and 110. The distance of closest approach between rigid units in the cell of Fig. 8 is 4.45 Å, a distance which is typical of the separation between stacked phenylenes on adjacent segments in similar systems, and the other distances of close approach are 5.49, 5.72 and 8.64 Å. This structure gives an area per chain of 22.7 Å^2. This compares extremely well with other structurally similar materials, Table IV.

The value of 22.7 Å^2 occupied by each aryl segment can be compared to the area occupied by an alkane chain. The lateral cross-sectional area in the expanded alkane lattice was found to be 19.2 Å^2 while the hypothetical cross-sectional area of an alkane chain in a typical amorphous phase (of density 0.85 g cm^{-3}) was calculated to be ∼22.0 Å^2. In other words, the aryl cross-sectional area is approximately the same as the area in a disordered alkane aggregate and larger than the area in the expanded alkane crystallites. This can only be consistent with the U conformation; for the molecule to assume an S configuration, the area occupied per segment in the aryl cell must be approximately twice that occupied per alkane chain (Fig. 4b).

It is therefore reasonable to conclude that the overall structure is comprised of layers ∼35 Å thick and that within each layer there are separate sub-layers of alkane and rigid rods. Pattern II is a chain axis projection of the rigid rod segment in the molecule which is only obtained when the rigid rod crystallites are aligned with the chain axis vertical. i.e. parallel to the electron beam. Finally, the crystals are also rotated around the needle (fiber) axis to give the observed structure. Importantly, this gives a projection between the planes marked A and B of 8.3 Å along the lath axis, Fig. 8. This is also identical to the layer line periodicity of Pattern I. Of course, as the crystallites twist around the lath axis in the fiber geometry, the chain axis projection is lost. Eventually this rotation brings chains normal to the incident electron beam and, also, the layer spacing (∼35 Å) into reflecting position. Moreover, this projection also brings a whole new set of crystal planes into reflecting position. These are the planes formed by the combination of the 8.3 Å periodicity along the needle axis with the 35 Å periodicity perpendicular to the needle (Fig. 9). This gives rise to the numerous reflections with a basic periodicity of 8.3 Å lying close to the meridion in the electron diffraction, which appear in x-ray diffraction as the family of reflections between 2θ of 10° and 14° and also the peak at 24.6° (3.61 Å).

Consider again the diffraction pattern in Fig. 7 and particularly the single crystal nature of the low angle reflection, Fig 7b. This implies that each needle consists of an array of highly regular, highly parallel layers. However, the arcing of the diffraction originating from

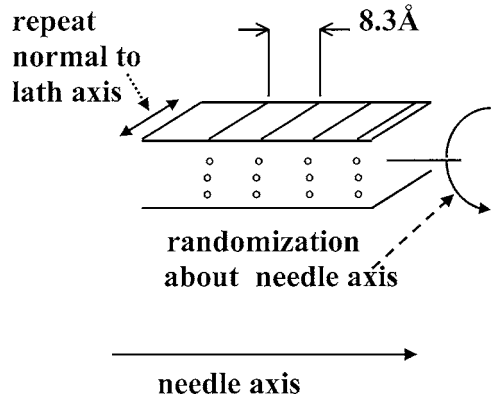

Figure 9 Schematic showing randomization around needle axis and origins of Pattern I reflections.

the rigid component suggests that each needle consists of a large number of rigid rod crystallites in a mosaic structure. Recall also that, when they did appear, spot patterns of the alkane lattice were found rather than arced or ring patterns. This can occur if either there are only small isolated alkane crystals, occasionally entering the electron beam, or, alternatively, if there is one large alkane single crystal covering the whole of the beam. The absence of alkane reflections in bulk x-ray diffraction, however, argues that the alkane material is essentially non-crystalline. Therefore, where they do appear, the alkane single crystal electron diffraction patterns are considered to arise from crystals which are too few and/or small to give bulk x-ray scatter, passing in and out of the electron beam. Such sites of alkane crystallization can reasonable be termed "incipient crystallites" which exist within an essentially disordered alkane component. However, to achieve a layering of ~35 Å, it is still necessary that layers of more-or-less extended alkane material must form, but, in this case, in an essentially disordered, non-crystalline structure. The hypothetical lateral cross-sectional of 22.0 $Å^2$ for an alkane chain in a typical amorphous phase can be compared with the observed 22.7 $Å^2$ for the rigid lattice to which it is physically attached and to the equilibrium 18.28 $Å^2$ in an unconstrained alkane crystal lattice (calculated from cell parameters in [4]). It is clear that overall crystallization of the system is controlled by packing of the rigid units. The mismatch in lateral areas between the aryl and alkane crystal lattices is probably the source of the frustration for the alkane crystallization.

The model being arrived at is therefore one of layers of crystallized aryl units alternating with layers of essentially disordered alkane units in which the crystallization of the alkane is almost completely frustrated. Any difference between rigid cell area and the smaller disordered alkane chain area must necessarily produce a strain across the interface between the rigid and alkane layers. Moreover, this will be cumulative with the lateral size of rigid crystal. Eventually, with increased growth of the rigid crystal, this strain will reach a point where it will become prohibitive to further growth of the rigid crystal. Similar such morphological effects have been reported before in homopolymers of low crystallinities, where a mismatch results from volume differences in the crystal phase and a higher volume disordered component [7]. Such situations lead to an upper bound in crystal size and to morphologies consisting of aggregates of numerous small crystallites of very small size, consistent with observations in the present case.

Some incipient crystallization of alkane material into an expanded orthorhombic cell is also clearly possible. It is noted that the cross-sectional area of this expanded alkane crystal lattice is then 16% smaller than that of the rigid cell. Whether the strain is produced by alkane crystallization or by the difference in area between the disordered alkane and the crystallized rigid segments, there is no reason to assume this will be accommodated by the interface isotropically. Such an anisotropy will tend to twist the interface. This is considered to be a possible origin of the observed rotation of the crystallites around the lath axis.

5. Summary

The dimer crystallizes in a needle-like morphology with the molecules aligned perpendicular to the needle axis. The needles are actually micro-fibers in which the internal structure is randomized about the needle axis. Alkane segments and rigid rod segments segregate as separate sub-layers. Alkane segments form an essentially non crystalline layer (although with some incipient crystallization) while the aryl units form a layer of small crystals arranged in a mosaic type of structure. The two sub-layers together form an overall, extremely well defined layer periodicity of ~35 Å.

The chain axis projection of the rigid component is a two dimensional monoclinic cell with a cross-sectional area of ~23 $Å^2$ per chain. This means that the alkane tails, to which the aryl segments are linearly connected, cannot interdigitate. In order to form the observed layering of ~35 Å, the molecules, therefore, adopt the U configuration.

Acknowledgements

We gratefully acknowledge G. G. Willson and D. Mederios of the Dept. of Chemistry of the University of Texas, Austin, for kindly supplying us the sample. The support of the MRSEC at the Polymer Science and Engineering Dept., University of Massachusetts is also acknowledged.

References

1. A. C. GRIFFIN, N. W. BUCKLEY, W. E. HUGHES and D. L. WERTZ, *Mol. Cryst. Liq. Cryst.* **64** (1980) 139.
2. D. CREED, J. R. D. GROSS, S. L. SULLIVAN, A. C. GRIFFIN and C. E. HOYLE, *ibid.* **149** (1987) 185.
3. A. C. GRIFFIN, M. L. STEELE, J. F. JOHNSON and G. L. BERTOLINI, *Nouveau Journal de Chemie* **3** (1979) 679.
4. C. W. BUNN, *Trans. Faraday. Soc.* **35** (1939) 482.
5. P. C. DAWSON and D. J. BLUNDELL, *Polymer* **21** (1980) 577.
6. J. BOON and E. P. MAGRE, *Die Makromolekulare Chemie* **126** (1969) 130.
7. A. J. WADDON, A. KELLER and D. J. BLUNDELL, *Polymer* **33** (1992) 27.

Received 21 April 2000
and accepted 31 May 2001